Continental Shelf Research, Vol. 3, No. 1, pp. 35 to 53, 1984.
Printed in Great Britain.

0278–4343/84 $3.00 + 0.00

Island sheltering of surface gravity waves: model and experiment

S. S. PAWKA,* D. L. INMAN* and R. T. GUZA*

(*Received* 6 *May* 1983; *in revised form* 3 *October* 1983; *accepted* 11 *October* 1983)

Abstract—A field experiment is used to evaluate a numerical model of the sheltering of gravity waves by islands offshore of the Southern California region. The sheltering model considered here includes only the effects of island blocking and wave refraction over the island bathymetry. Wave frequency and directional spectra measured in the deep ocean (unsheltered region west of the islands) were used as input to the sheltering model and compared with coastal observations. An airborne L-band synthetic aperture radar was used to image the directional properties of the waves in the deep ocean. In addition to the unsmoothed spectra, a unimodal directional spectrum model obtained from fits to the radar spectra was also employed to suppress the high noise level of this system. Coastal measurements were made in about 10 m depth at Torrey Pines Beach with a high resolution array of pressure sensors. The model predictions and data at Torrey Pines Beach agree well in a limited frequency range (0.082 to 0.114 Hz) where the unimodal deep ocean model is appropriate. The prediction that unimodal northern swell in the deep ocean results in a bimodal directional spectrum at Torrey Pines Beach is quantitatively verified. The northern peak of the bimodal spectra is due to waves coming through the window between San Clemente and San Miguel-Santa Rosa Islands. The southerly peak is due to wave refraction over Cortez and Tanner Banks. For lower frequency waves, the effects of strong refraction in the island vicinity are shown qualitatively. Refraction can theoretically supply up to approximately 10% of the deep ocean energy that is otherwise blocked at this site. The modifications of the island shadows due to wave refraction become theoretically negligible for wave frequencies >0.11 Hz. Also, local wave generation effects, which are not included in this sheltering model, are shown to be occasionally important for waves with frequencies >0.12 Hz.

INTRODUCTION

THE presence of the Channel Islands (Fig. 1) has long been recognized as a dominant factor in the Southern California coastal wave climate (ARTHUR, 1951). The islands provide significant shelter to the coast from deep ocean surface gravity waves. The island shadow regions are physically blocked from waves impinging directly on the subaerial island boundaries. The wave energy is either dissipated in the islands' surf zones or reflected back out into the deep ocean. However, there are many processes which may spread wave energy into the islands' lee. These include wave refraction or scattering over the island shoals, wave diffraction, wave–current interaction, and nonlinear effects. A model is developed here which numerically evaluates the effects of wave refraction and island blocking. These mechanisms are thought to be the dominant linear effects for the sheltering of low frequency wind generated waves over the space scales of the distance from the islands to the coast (~100 km). The numerical model is then tested with field measurements of the wave field.

* Shore Processes Laboratory, Scripps Institution of Oceanography, University of California, San Diego, La Jolla, CA 92093, U.S.A.

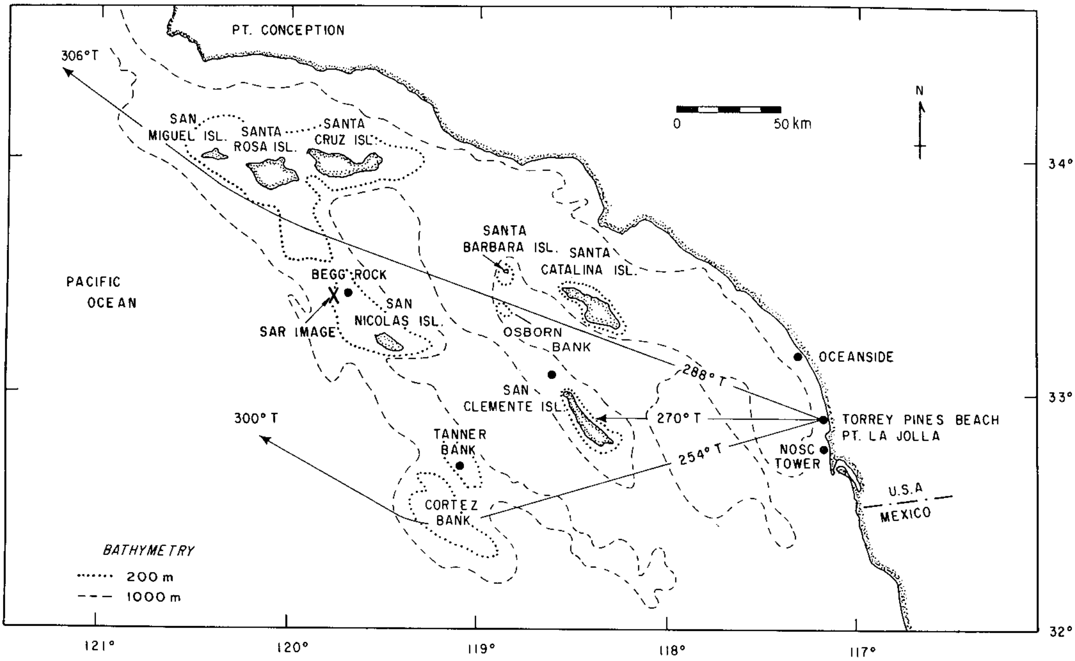

Fig. 1. Schematic map of the Southern California borderland showing the surface sensor sites (dots) and location of the 'deep ocean' SAR images (X). Also shown are three rays for 0.059 Hz waves incident to TPB.

The sheltering effects of islands have been studied previously. ARTHUR (1951) used visual observations along the Southern California coast to indicate shadows of the Channel Islands in the presence of south swell. Arthur concluded that wave refraction over the island shoals dominates the effects of diffraction or wave–current interactions in modifying the island shadow. EMERY (1958) also visually observed reduced wave heights in the lee of the Channel Islands. Several studies, including HOM-MA *et al.* (1966) on the Niigata coast (Japan), WILSON *et al.* (1973) in the Caribbean, and PAWKA (1983) in Southern California, indicate the qualitative effects of refraction in the island sheltering process. However, none of these studies attempt to model the full transformation of the frequency–directional spectrum. The primary information that is lacking is the synoptic measurement of the directional spectra in the exposed (deep ocean) and sheltered regions.

The work presented here is based on an extensive field measurement program quantifying the island sheltering processes in the Southern California region. This study was undertaken as part of the Seasat West Coast Experiment. The measurements included *in situ* estimates of the wave frequency spectrum along the coast and in the 'deep ocean' (relatively unsheltered region offshore of the islands). Wave directional spectra were measured in about 10 m depth at Torrey Pines Beach (TPB) with a high resolution linear array. An airborne L-band synthetic aperture radar (SAR) was used to sample the deep ocean directional spectrum estimates. SAR data were sampled on only 2 days of the month-long experiment and fidelity problems with these spectra (discussed in PAWKA *et al.*, 1980) limited the frequency range of useful data-model comparisons.

The deep ocean estimates of the frequency–directional spectrum were transformed by the island refraction/blocking model to yield deep water predictions just offshore of TPB and Oceanside (defined as local deep water). The array measurements of the frequency–directional spectrum at TPB were refracted out over the local shelf bathymetry for direct comparison with the predicted spectrum in local deep water. The comparisons are made in local deep water, rather than at the shallow water sites, because in local deep water the directional features of the island shadows are undistorted by further refraction over the shelf. The predicted and observed spectra are in good agreement at TPB for the limited range of frequencies which have reasonably accurate deep ocean directional spectrum estimates. The full range of experimental frequencies are discussed to highlight the critical need for accurate, high resolution directional spectra in the deep ocean for use in wave prediction on a sheltered coast. The comparison results are inconclusive at Oceanside, a site which is extremely sensitive to noise level problems in the deep ocean spectra.

ISLAND SHELTERING MODEL

Methodology

A numerical model is used to quantify the processes of wave refraction over the island shoals and blocking (ray capture) by the island boundaries. This model employs the method of refraction of a continuous spectrum which has been used by numerous investigators (MUNK *et al.*, 1963; COLLINS, 1972). The method is based on the conservation of $E(k)$, the wavenumber spectrum, along a ray (LONGUET-HIGGINS, 1957; PHILLIPS, 1977). This result requires a linear wave field, no sources or sinks of wave energy, slow variation of the bathymetry and wave amplitude, and no horizontal current shears. A transformation to the variables α (propagation direction) and f (frequency) yields

$$C^2 nE(f, \alpha) = \text{constant along a ray}, \tag{1}$$

where C is the wave phase speed and n is the group/phase speed ratio.

The ray paths were calculated over a digital representation of the bathymetry with the use of a numerical program developed by DOBSON (1967). This program integrates the fundamental ray equations (MUNK and ARTHUR, 1952) for the solution of the ray paths. The paths were constructed from coastal sites through the island shoals out into the deep ocean (Fig. 1). Refraction around Pt. La Jolla was also considered for the wave field at TPB. Coarse grids with 480 m spacing covered the broad regions between San Nicolas and Santa Rosa Islands and the Cortez and Tanner Banks. The bathymetry at Osborn Bank and both edges of San Clemente Island were simulated with grids of ~250 m spacing. The grids covered all bathymetry down to depths of 250 m.

The method of refraction of continuous spectra has particular advantage over the monochromatic (ray convergence) method when patching together results from many grids. The final result of the refraction analysis is a map of local directions into deep ocean directions for each coastal location. The analysis was carried out for a local directional bandwidth of 0.1° for rays projecting to relatively shallow portions of the island shoals and 0.2° for the remaining sectors. An angle difference of 0.1° at TPB projects to a horizontal separation of 150 to 300 m at the island grids. This separation range is roughly equivalent to the range of deep water wavelengths of waves of interest in this study. The fine resolution spectrum can be thought of as a smoothed version of the true (continuous) spectrum

$$E_{tp}(f, \alpha_{tp}) = \frac{1}{2\Delta_{tp}} \int_{\alpha_{tp}-\Delta_{tp}}^{\alpha_{tp}+\Delta_{tp}} E'_{tp}(f, \alpha'_{tp})\, d\alpha'_{tp}, \tag{2}$$

where $E'_{tp}(f, \alpha'_{tp})$ is the true spectrum at TPB, the subscript *tp* denotes TPB and $2\Delta_{tp}$ is the fine resolution bandwidth. All discussion of theoretical coastal spectra (or coastal response) will be in reference to local deep water (off the shelf) conditions and the factors C^2n (equation 1) cancel. Equation (2) can therefore be rewritten

$$E_{tp}(f, \alpha_{tp}) = \frac{1}{2\Delta_{tp}} \int_{F^{-1}(\alpha_{tp}-\Delta_{tp})}^{F^{-1}(\alpha_{tp}+\Delta_{tp})} E_{do}(f, \alpha_{do}) \frac{d\alpha_{tp}}{d\alpha_{do}} \, d\alpha_{do}, \tag{3}$$

where $E_{do}(f,\alpha_{do})$ is the deep ocean spectrum, the angles α_{tp} and α_{do} are related by the transformation $\alpha_{tp} = F(\alpha_{do})$. If $d\alpha_{tp}/d\alpha_{do}$ is relatively constant over the integration range then equation (3) is approximated by

$$E_{tp}(f, \alpha_{tp}) \cong \frac{1}{\Delta_{do}} \int_{F^{-1}(\alpha_{tp}-\Delta_{tp})}^{F^{-1}(\alpha_{tp}+\Delta_{tp})} E_{do}(f, \alpha_{do}) \, d\alpha_{do}, \tag{4}$$

where

$$\Delta_{do} = |F^{-1}(\alpha_{tp} + \Delta_{tp}) - F^{-1}(\alpha_{tp} - \Delta_{tp})|.$$

The algorithms were tested successfully against analytic solutions for simple bathymetry.

The integral of equation (4) is numerically evaluated to determine the coastal directional spectrum. However, the weighting of the spectrum in this integral is only an approximation and may cause considerable error if there is a significant curvature in the map $\alpha_{tp} = F(\alpha_{do})$. Caustics stemming from the island shoals cause discontinuities in the slope of the relationship $\alpha_{tp} = F(\alpha_{do})$. Direct application of equation (4) assumes that the singularities in $d\alpha_{tp}/d\alpha_{do}$ are localized and integrable. The possible errors are also a function of the smoothness of $E_{do}(\alpha_{do})$ over Δ_{do} (which is related to Δ_{tp} by the transformation curve). An error analysis was performed assuming smooth functions for the structure of caustics in the angle maps. The expected errors due to the approximation ranged from 10 to 20%, for smooth caustics associated with a single shoal, to 200 to 300% for complicated refraction over multiple shoals. However, <1% of the total aperture is expected to have these large errors.

The fine scale (0.1 to 0.2°) values of $E_{tp}(f, \alpha_{tp})$ were averaged into 1° directional bands. Rays which intercept the islands are terminated which leaves gaps in the coastal directional spectra. Therefore, the 'blocking' effect of the islands is imbedded in the model.

Wave refraction analysis was also used to transform the shallow water coastal measurements into local deep water spectral estimates. Refraction grids with spacing of about 50 m were developed for the coastal sites at TPB and Oceanside. The ray paths were constructed from the sensor locations out into local deep water. The directional spectra analyzed from the linear array at TPB were used directly in the transformation of finite depth measurements into local deep water values using the techniques described by PAWKA *et al.* (1980).

Theoretical wave transformations

The energy responses at TPB and Oceanside are shown as a function of deep ocean direction for several wave frequencies in Fig. 2. The response is defined as, e.g., $E_{tp}(f)/E_{do}(f)$, where

$$E_{tp}(f) = \int_{\alpha} E_{tp}(f, \alpha) \, d\alpha \tag{5}$$

and the deep ocean (*do*) spectrum is defined in the same fashion. Due to the fact that the islands are relatively close to the coast (~100 km), even the small separation between TPB and Oceanside (~30 km) clearly results in substantial variations in the coastal look angles directed toward major island features (e.g., San Clemente Island in Fig. 1). As a result, there

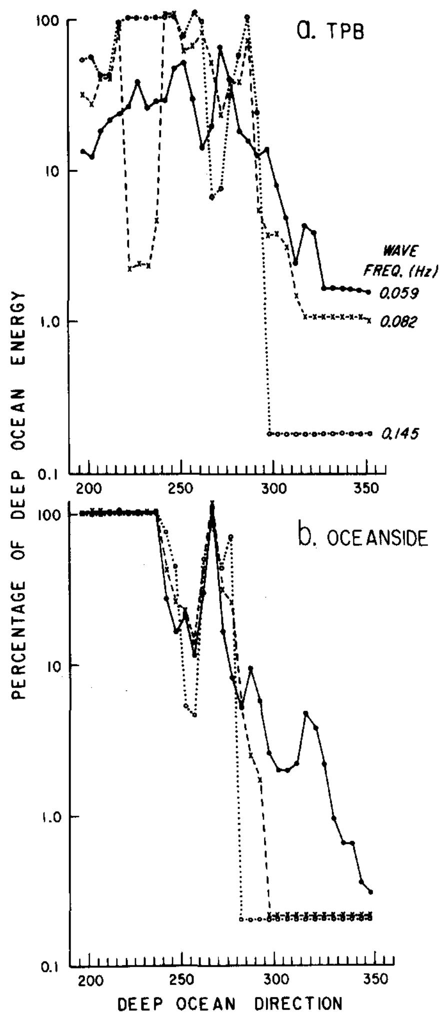

Fig. 2. Wave energy response at (a) TPB and (b) Oceanside vs deep ocean direction. The values given are for the wave energy ratio coastal/deep ocean for 5° rectangular spreads in deep ocean directions. The flat segments of the curves at high north angles (300 to 350°T) are an artifact of the averaging in the model.

is a marked difference in the response functions at the two coastal sites. The variation of the responses with wave frequency at a particular site is due to the wavelength dependence of the refraction process. If only island blocking is important, the blocked sectors are sharply defined, and the response functions are frequency independent. The strong frequency dependence of the response functions at TPB, which is indicative of the importance of island refraction effects, is due to the relatively large exposure at this site to Cortez and Tanner Banks.

Nearly all of the low frequency directional spectrum at TPB is affected to some extent by the bathymetry either in the Channel Islands or Pt. La Jolla regions. There are no 'open windows' (i.e., topographically unaffected quadrants) of exposure to the deep ocean

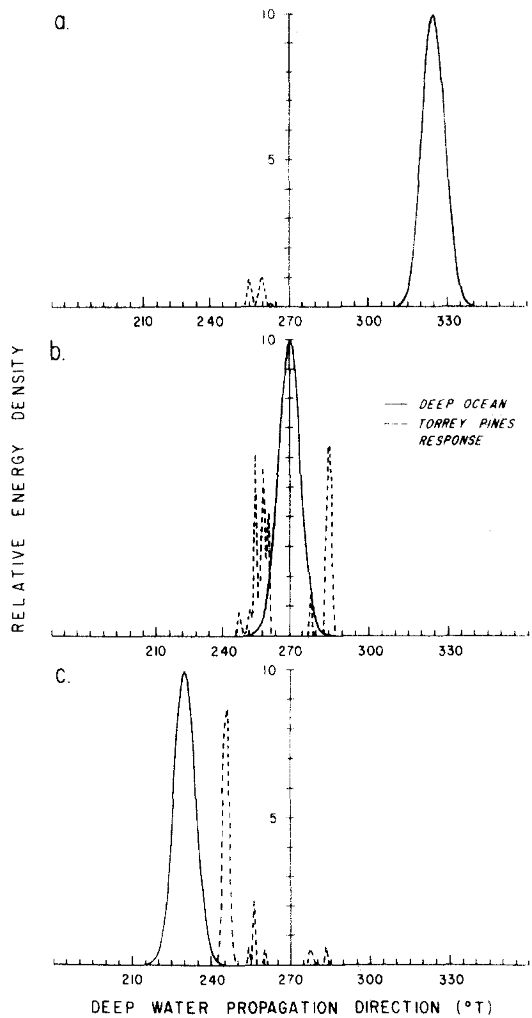

Fig. 3. Theoretical directional responses at TPB for 0.059 Hz waves and for three deep ocean spectral forms (a, b, c). The transformations were computed using the island refraction/blocking model. A null result is predicted for the shadowed quadrants (e.g., the San Clemente Island shadow centered on 270°T).

directional spectrum for wave frequencies <0.06 Hz. Refractive effects smooth the low frequency response function (Fig. 2) and provide a fairly significant response to all sectors of the deep ocean spectrum. The most important feature of the refraction effects is the response to low frequency waves with deep ocean angles 300 to 330°T, which is a sector that is completely blocked by the linear island shadows (Fig. 1). Although the response is only 1 to 10%, that is significant because of the strong dominance of these directions in the annual wave climate (NATIONAL MARINE CONSULTANTS, 1960).

The higher frequency response functions at TPB have sharper delineation of the windows to the deep ocean due to the decreasing importance of refractive effects. For example, the definition of the "northern quadrant window", centered on 285°T, sharpens with increasing wave frequency (Fig. 2). The energy refracted to TPB for waves with $\alpha_{do} \geqslant 295°T$ is insignificant for frequencies >0.10 Hz. Also, a significant spread of southerly directions are completely open at high wave frequencies.

The characteristics of the directional spectra at the coast are greatly affected by the presence of the borderland islands and shoals. The 0.059 Hz directional responses at TPB to three unimodal deep ocean directional spectra are shown in Fig. 3. Energy from a large range of deep ocean directions refracts into coastal sectors which point to the shoals (shoal apertures). In this way, these shoal regions appear as 'diffuse sources' of wave energy, regardless of the structure of the deep ocean directional spectrum. The major refractive sources are Cortez and Tanner Banks (250 to 259°T), the southern shoals of San Clemente Island (261 to 263°T), and the shoals of the northern quadrant window (278 to 290°T).

The relative energy provided by these refractive sources varies as a function of the deep ocean directional spectrum. Figure 4 shows the relative energy of the refractive sources, as well as the directionally integrated response at TPB, for various unimodal northern swell sources. The northern window quadrant peak and the banks quadrant peak (250 to 269°T) are comparable in energy level for a wide range of deep ocean spectral conditions. The relative strength of the banks quadrant peak, which has southerly directions at TPB, is seen to increase for deep ocean mode angles >305°T (Fig. 4b, b'), although this involves only a small percentage of the unsheltered energy (Fig. 4a, a'). Very high angle north swell is shown in Fig. 3a to primarily approach TPB from southerly directions. This is due to strong refraction over Cortez Bank.

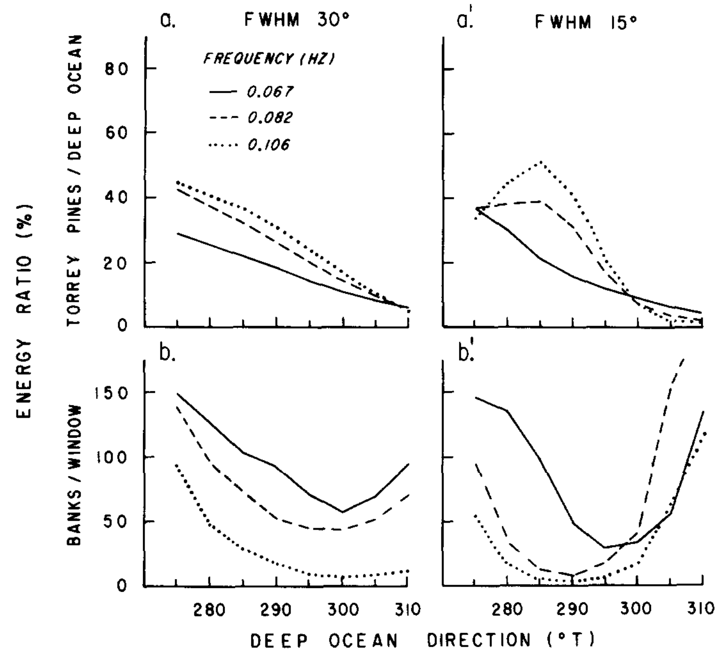

Fig. 4. (a, a') Ratio of band energy at TPB to the deep ocean value. (b, b') Ratio of banks quadrant (250 to 269°) energy to the northern window quadrant (270 to 295°T) energy at TPB. These ratios are theoretical results obtained from the refraction/blocking model and are expressed as a function of mode direction for two unimodal deep ocean spectral forms. FWHM denotes the full width at half maximum of the deep ocean modes.

The presence of the borderland islands restricts the possible wave approach angles at the coast. In fact, neglecting local wave generation, the wave energy at TPB should be contained in a few relatively narrow directional sectors, reducing the potential diversity of the local directional spectrum. On the other hand, the blocking and refraction effects may at times complicate the coastal wave conditions. The examples shown in Fig. 3 illustrate a common bimodal or even trimodal directional response at TPB to simple unimodal deep ocean spectra. The only unimodal directional response at this site (at low frequency) occurs under the conditions of very high angle northern swell (Fig. 3). PAWKA (1983) showed a smearing of these sharp island features in the coastal directional spectra due to local generation for wave frequencies >0.13 Hz.

The refraction process (i.e., topographic effects other than simple blocking) appears to be important to the response functions at Oceanside only for the lowest wave frequencies (Fig. 2). At higher frequencies, the windows and blocked sectors are sharply defined. This is due to the relatively narrow exposure at this site to Cortez and Tanner Banks. In general, Oceanside has a much reduced response to northern swell as compared to TPB. However, Oceanside is fully exposed to the major southern swell sources ($\alpha_{do} \sim 220$ to 245°T), while TPB is locally sheltered by Pt. La Jolla. Oceanside's major window between the islands is around 265 to 275°T, which is a relative trough in the average annual deep ocean spectrum (estimated from hindcast data by NATIONAL MARINE CONSULTANTS, 1960), but can be an energetic sector during periods of local storm activity associated with relatively severe winters.

EXPERIMENTAL SET-UP

Field measurements for testing the island sheltering model were acquired during the month of March 1977 as part of the SEASAT West Coast Experiment. A widespread coverage of the wave field in island and coastal regions was obtained with a variety of *in situ* and remote sensors (Fig. 1). The measurements discussed here are a subset of the full complement of the experiment. SHEMDIN (1980) discusses the overall scope of the measurements and scientific goals of the West Coast Experiment. A more detailed description of the sensors used here is given in PAWKA (1982).

Measurements in the island vicinity

Accurate measurements of the deep ocean (relatively unsheltered) frequency–directional spectrum were crucial for the success of this experiment. These data were sampled by a combination of remote and *in situ* systems. The 'deep ocean' frequency spectra were measured with a Datawell waverider which was moored in a position about 24 km northwest of San Nicolas Island (near Begg Rock). This site is in a mean depth of 110 m and is fully exposed to deep ocean waves in the directional range 180 to 320°T. The Pacific Missile Test Center maintained this buoy, collected the data, and performed the spectral analysis. Twenty minute data runs were sampled daily at 0100 and 1130 PST.

The deep ocean directional spectra were obtained from an L-band SAR flown by the Jet Propulsion Laboratory aboard a CV-990 aircraft. The SAR images used in the analysis were taken just west of the Begg Rock waverider. The SAR analysis yields a directional distribution for each wave frequency and these were then normalized by the waverider frequency spectra to yield the frequency–directional spectrum. Comparative studies of this SAR and the TPB high resolution linear array show that the SAR spectra yield good estimates of the location and width of the primary directional mode (PAWKA *et al.*, 1980). However, the SAR did not reliably image small secondary peaks and also displayed a relatively high background 'noise' level in the spectra. The details of the SAR sampling and analysis are given in Pawka *et al.* (1980).

A Baylor gauge and an Endeco electromagnetic current meter were operated by the Shell Development Company on an oil platform on Tanner Bank. The current meter was analyzed for 'dominant' wave direction while the Baylor gauge yielded frequency spectra. The site has roughly the same wave exposure as Begg Rock and has a mean depth of 61 m. These data were not available during the SAR overflight days. Another Datawell waverider was maintained at a position 10 km northwest of San Clemente Island in deep water (600 to 700 m). This site is partially sheltered by the islands and is approximately midway between Begg Rock and the coastal stations. Data from this buoy were sampled continuously during periods of intense experimental activity. Aerial photographs, which were used for determining dominant wave direction, were taken from several aircraft during the experimental month. Descriptions of the flight patterns and aircraft are given in Shemdin (1980).

Surface anemometers were located at San Nicolas Island, San Clemente Island, and at the Naval Ocean Systems Center (NOSC) tower in Mission Beach. Three hour averages of wind speed and direction were obtained from each site.

Coastal waves measurements

A 400 m linear array of five pressure sensors was maintained at TPB for the measurement of high resolution frequency–directional spectra. The high directional resolution was required to resolve the complicated structure due to the island blocking and refraction effects. The shelf at TPB is nearly planar (Pawka, 1983), and homogeneity of the wave field is expected over the array's length. The 400 m length was chosen for resolution of the San Clemente Island shadow at 0.07 Hz, the energetic mode of northern swell. This requires resolution of two narrow peaks separated by 8° in 10 m depth. The 1–2–4–5 configuration of the sensor lags (unit lag = 33 m) was determined by Pawka (1982) to be a reasonable array.

Various surveying techniques were used to establish the array sensor positions to within 1 m. This position uncertainty corresponds to an orientation error of about 2° for the shortest lag and $<1°$ for the longer lags. The absolute orientation of the array was based on the sensor positions relative to two upper beach bench marks. Discrepancies of $\pm 1°$ in the magnetic heading of the line between these bench marks causes an uncertainty of ± 1.5 to 3.0° in deep water directions.

The linear array provides useful directional spectra in the frequency range 0.05 to 0.15 Hz. Resolution problems establish this lower limit while the high frequency cutoff is due to the onset of aliasing. The frequency–directional spectra are transformed out into local deep water using a linear refraction model. The local deep water estimates are suitable for direct comparison with the sheltering model predictions of coastal wave spectra. An attempt was made to synchronize the coastal wave predictions and measurements. Wave energy with frequencies considered in this study takes from 4 to 12 h to travel from Begg Rock to TPB. Where possible, this time shift was accounted for in the data analysis.

Several high resolution directional spectrum estimators are used in the array analysis. The Maximum Likelihood Method (MLM; Capon, 1969) is the primary estimator employed. This estimator has been shown to yield excellent qualitative features (peak locations and widths) of spectra dominated by narrow modes (Regier, 1975; Pawka, 1983). However, the method is found to be lacking in the quantification of these spectral features. Therefore, two additional estimators are also considered in this study. The first is an iterative modified form of the

MLM (IMLM) which attempts to deconvolve the spectral smearing effects. Secondly, a minimum square window error technique (MSEM) is also utilized. These two estimators are discussed at length in PAWKA (1983) and have better expected performance than the MLM in certain estimation problems. This will be further discussed when the results of the estimators are intercompared.

A single pressure sensor was maintained in a depth of 7.4 m at Oceanside. This sensor was part of a network of coastal wave stations which are monitored by the Nearshore Research Group at Scripps Insitution of Oceanography. These stations were sampled consecutively for data runs of 17.1 min duration. The normal sampling frequency of 2 runs per day was increased to about 6 to 10 during the SAR overflight days. The predicted directional spectra obtained from the sheltering model for Oceanside were used to transform the shallow water frequency spectra into local deep water. This supplied a directionally integrated energy check on the coastal predictions at this site.

DATA-MODEL COMPARISONS

Wave measurements were sampled at the surface sites throughout the month-long experiment. SAR imagery, which provides the deep ocean directional information necessary to test the island sheltering model, was sampled only on 25 and 28 March. Emphasis here will be placed on the data obtained on these two days. The frequency spectra obtained from the Begg Rock waverider and the SAR directional spectra, $E_r(\alpha)$, sampled near this location were combined to yield estimates of the deep ocean wave conditions. The SAR spectra were sampled slightly west of the Begg Rock waverider and this sheltering was accounted for by the refraction model (10 to 20% effect) to yield a 'deep ocean' frequency spectrum. The frequency spectra measured at TPB, Oceanside, and Begg Rock on 25 and 28 March are shown in Fig. 5. In general, the coastal spectra significantly underlie the deep ocean spectrum. This is qualitative evidence of the island sheltering effects. The exceptions to this general trend will be discussed in detail below. The data-model comparisons are obtained by transforming the deep ocean measurements of the frequency–directional spectra through the sheltering model to predict the local deep water coastal wave spectra. These predictions are then compared to the local deep water estimates obtained from the coastal sites. Predictions were also made with unimodal approximations (Table 1) in an attempt to suppress the effects of high noise levels in the SAR directional spectra. The frequency spectrum comparisons are detailed in Table 2. These results, and the directional comparisons at TPB, are discussed in terms of three ranges in frequency.

Low frequency (0.059 *to* 0.074 Hz)

The low frequency range is characterized by significant southern and northern components in the deep ocean spectra. The SAR directional spectra in this frequency range imaged near Begg Rock generally have a disordered appearance with only a vague indication of the northern and southern swell peaks. An example low frequency SAR spectrum is shown in Fig. 6 along with the predicted response and measured directional spectrum at TPB. The predicted and measured values of the mode direction agree well for this example, but do not generally hold true for the low frequency comparisons. PAWKA et al. (1980) found poor performance of the SAR system at these low frequencies in a direct comparison with the array at the TPB site. The data-model energetic comparisons (listed in Table 2) are highly scattered for both the TPB and Oceanside sites. We feel that neither the SAR spectra nor the

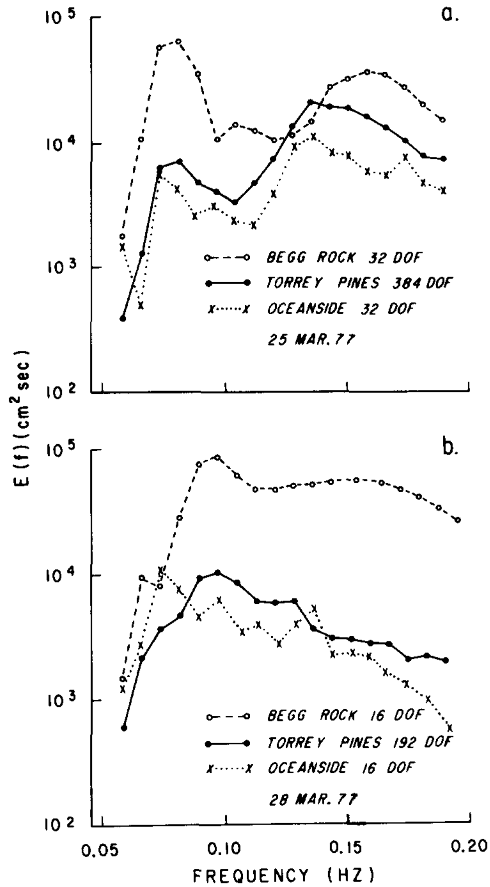

Fig. 5. Average frequency spectra for Begg Rock (deep ocean), TPB, and Oceanside. The coastal spectra have been refracted out into local deep water. DOF indicates the degrees of freedom of the spectral estimates.

Table 1. Mode parameters for the unimodal distribution representations of the SAR spectra. α_m is the best-fit mode direction while $\Delta\alpha_m$ is the full width at half maximum of the cos power distribution (both in degrees). The residual (%) is defined: residual $= \Sigma_\alpha (E_u(\alpha) - E_r(\alpha))^2 / \Sigma_\alpha E_r^2(\alpha)$, where $E_r(\alpha)$ is the SAR spectrum and $E_u(\alpha)$ is the unimodal approximation

	25 March, 1977			28 March, 1977		
Frequency (Hz)	α_m	$\Delta\alpha_m$	Residual	α_m	$\Delta\alpha_m$	Residual
0.059	248	10	51.4	280	14	48.9
0.067	282	14	41.7	220	16	57.0
0.074	299	65	20.8	320	10	51.3
0.082	306	10	42.2	294	12	50.8
0.090	302	35	25.5	297	14	33.3
0.098	298	50	20.4	297	22	32.8
0.106	292	30	22.3	289	30	36.1
0.114	283	10	41.3	295	12	45.7
0.121	280	35	33.1	297	20	37.3
0.129	302	90	9.8	281	35	30.7
0.137	299	90	5.8	290	90	13.5
0.145	298	90	6.8	280	90	18.1

Table 2. Ratio (%) of measured band energy at the coastal sites (deep water) to the values predicted with the island refraction/blocking model. The comparisons with the SAR spectrum, $E_r(\alpha)$, and the unimodal approximation, $E_u(\alpha)$, as estimates of the deep ocean directional spectrum are listed

	Torrey Pines Beach				Oceanside			
	$E_r(\alpha)$		$E_u(\alpha)$		$E_r(\alpha)$		$E_u(\alpha)$	
Frequency (Hz)	25 Mar	28 Mar	25 Mar	28 Mar	25 Mar	28 Mar	25 Mar	28 Mar
0.059	110.0	209.0	49.6	133.0	198.0	224.0	400.0	690.0
0.067	51.5	111.0	40.6	64.1	11.3	93.5	49.8	3.24
0.074	42.0	183.0	58.6	150.4	30.6	372.0	86.8	1000.0
0.082	52.9	54.8	240.0	87.7	30.3	86.7	565.0	1270.0
0.090	60.1	60.2	101.0	97.8	40.9	29.6	157.0	266.0
0.098	123.0	41.4	175.0	58.8	91.8	23.9	283.0	323.0
0.106	73.0	40.0	85.4	45.0	60.7	18.7	174.0	44.9
0.114	97.4	42.8	62.8	70.5	48.3	24.6	128.0	712.0
0.121	228.0	37.6	178.0	68.1	111.0	16.3	134.0	305.0
0.129	330.0	32.4	464.0	29.6	253.0	24.6	447.0	30.9
0.137	433.0	17.9	492.0	19.7	249.0	32.7	380.0	50.6
0.145	232.0	13.9	243.0	12.9	98.7	11.0	145.0	13.5

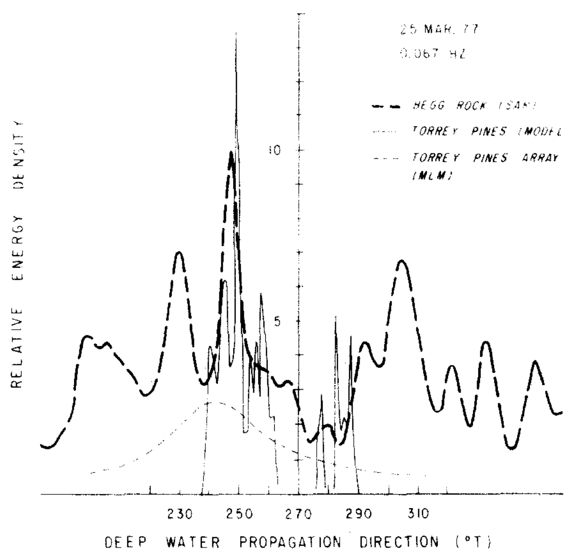

Fig. 6. Comparison of predicted and measured (MLM) directional spectra at TPB. The predicted spectrum was generated using SAR directional inputs into the island refraction/blocking model. The measured coastal spectrum has been refracted into local deep water for the comparisons. The curves are normalized by a constant factor. The band energies are 1.8×10^3 cm^2 s^{-1} at Begg Rock and 4.1×10^2 cm^2 s^{-1} at TPB.

unimodal approximations are of sufficient quality to test the sheltering model in the low frequency range. This is unfortunate because the refraction process was shown theoretically to be most significant for low frequency waves.

There are some observed features in the low frequency TPB directional spectra that are qualitatively consistent with the predicted island refraction effects on northern swell. The coastal low frequency spectra of 5, 9, and 10 March show no indication of deep ocean southern swell ($\alpha_{do} \lesssim 240°$T). The low frequency modal directions obtained from the Tanner Bank current meter were all in the range 305 to 320°T for these three days. Also, aerial photographs taken from two independent systems showed dominant deep ocean swell angles of 306 and 316°T on 10 March.

The 0.059 Hz directional spectrum sampled at TPB on 5 March is shown in Fig. 7. The central trough aligns with San Clemente Island, a feature discussed in detail by PAWKA (1983). The directions of the strong southern mode (253°T) are consistent with the Cortez Bank refractive energy source (Fig. 3). At higher frequency this southern mode is reduced in relative importance (in qualitative agreement with model predictions, Fig. 4b, b′) and the mode direction shifts to about 258°T. This directional shift is also predicted by the model response to northern swell.

The TPB low frequency directional spectra of 9 and 10 March have similar structure to the 5 March spectra. The energetic ratio of the banks quadrant peak to the northern window quadrant peak, as well as the relative energies at TPB and Oceanside on 5, 9, and 10 March (all listed in Table 3) are consistent with the relatively narrow (15 to 30°) deep ocean peak with mode directions of 305 to 315°T. There is a change in the energetic ratios from 5 to 9 and 10 March which is consistent with the northern shift in deep ocean directions on the latter two days observed at the Tanner Bank current meter. These data do not provide quantitative verification of the island sheltering model. However, we suggest that they provide strong evidence for the importance of the refractive process in the low frequency region, and are qualitatively consistent with the sheltering model and the available wave data.

Mid-frequency (0.082 *to* 0.114 Hz)

The deep ocean SAR spectra in the mid-frequency range are dominated by a relatively narrow (10 to 30°) peak around 280 to 305°T. The sheltering model tends towards over-prediction of the coastal energy values with the use of the SAR spectra as deep ocean inputs (Table 2). However, there is a reduction of the scatter relative to the low frequency range. A plot of the Begg Rock SAR spectrum and the predicted response at TPB for 0.090 Hz waves

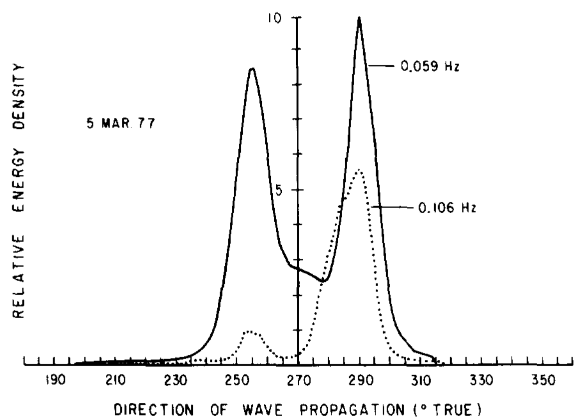

Fig. 7. Directional spectrum estimates (IMLM) obtained from the linear array at TPB. The spectra have been refracted out into local deep water. The associated cross-spectra have 800 d.f. The measured band energies are 9.0×10^3 cm^2 at 0.059 Hz and 1.9×10^3 cm^2 s^{-1} at 0.106 Hz.

Table 3. Comparisons of measured and theoretical values of two coastal energetic ratios. Ba/NWQ is the ratio at TPB of the banks quadrant (250 to 269°T) energy to the northern window quadrant (270 to 295°T) energy. OS/TPB is the ratio of energy at Oceanside and TPB (local deep water). The ratios are in percent and the analysis is for 0.059 Hz. The angles given are for the theoretical deep ocean spectra with the full width at half maximum indicated in parentheses

	Ba/NWQ	OS/TPB
Date (March 1977)	Measured	
5	88.8	24.3
9	119.0	56.0
10	148.0	47.8
Mode angle	Theoretical	
305 (20°)	55.1	38.5
310 (20°)	109.0	62.0
315 (20°)	258.0	88.3
305 (30°)	68.2	47.3
310 (30°)	90.5	50.9
315 (30°)	147.0	68.1

on 25 March is compared to the local measured directional spectrum in Fig. 8a. For illustrative purposes, the linear array's response to the predicted spectrum was calculated and is compared to the measured spectrum in Fig. 8b. This 'smeared prediction' agrees well with the measured spectrum for angles >250°T. However, there is an excess of predicted energy density in the sector $180°\mathrm{T} < \alpha_{tp} < 250°\mathrm{T}$, most likely due to the relatively high noise level in the SAR spectrum. This bias in the southern quadrant is seen throughout the mid-frequency range and is the probable cause of the overpredicted coastal energy values.

The smeared coastal response to the unimodal deep ocean approximation for 0.090 Hz on 25 March is compared with the measured spectrum in Fig. 8c. The predicted band energy is within 5% of the measured value for this comparison. Also, the predicted response locates well the two primary directional modes. The more smeared appearance of the measured spectrum may be due to a low background level in the southern quadrant that is not accounted for by the unimodal distribution. The northern swell unimodal model generally underpredicts the southern quadrant energy density. However, the average unimodal prediction bias for band energy in this frequency range is only 3% for the TPB comparison, which indicates that the mishandling of the southern quadrant is not serious at this site. The scatter of the individual comparison values is within the expected range for the ratio of statistically independent spectral estimates with the appropriate degrees of freedom. It is expected that the unimodal deep ocean approximation would be most appropriate in the mid-frequency range due to the relative unimportance of southern swell (PAWKA, 1982) or local wind effects (discussed later) in this range.

The structure of the TPB spectra in the mid-frequency range is characterized here by the energetic ratio of the banks quadrant peak to the northern window quadrant peak. The predicted values of this parameter are listed in Table 4 along with the measured values estimated with three spectral techniques. On the basis of model testing, the IMLM and MSEM spectra

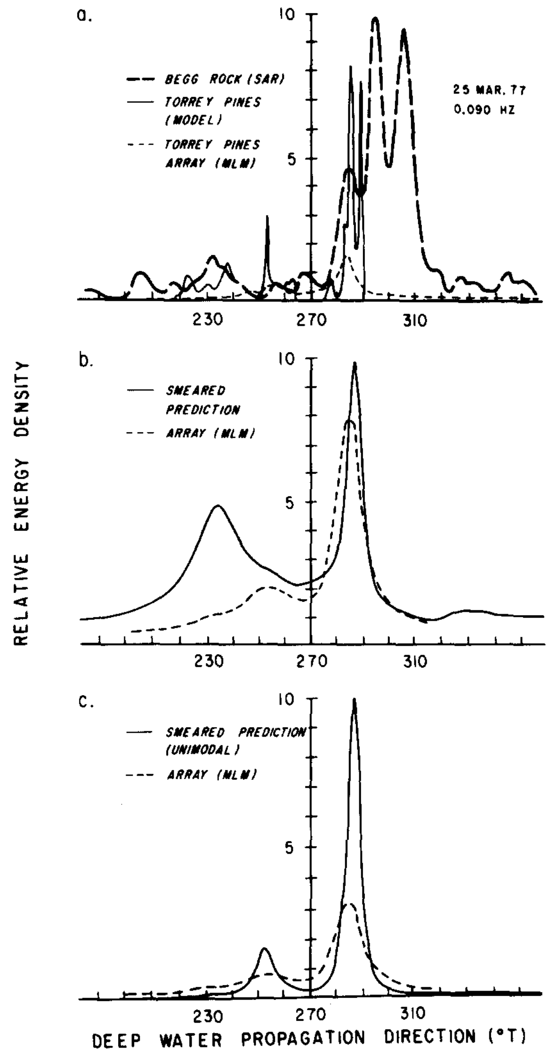

Fig. 8. Comparisons of predicted and measured spectra at TPB. The predicted spectra were generated by SAR directional spectra inputs from the island refraction/blocking model. Shown are the comparisons of the TPB array spectra with (a) prediction with the raw SAR spectrum as the input, (b) smeared prediction (MLM filter) with the raw SAR spectrum as the input, and (c) smeared prediction with the unimodal approximation as the input. The spectra are normalized by a constant factor. The measured band energies are 3.5×10^4 cm^2 s^{-1} at Begg Rock and 4.8×10^3 cm^2 s^{-1} at TPB.

are expected to be more accurate estimators (Pawka, 1983). The SAR spectra uniformly overpredict the relative energy in the banks quadrant, because of the noise problems discussed above. The unimodal predictions show close average comparisons with the measured values, particularly those made with the IMLM spectra. There is a significant amount of scatter in the individual band comparisons, which we have not attempted to statistically model, but do note that the unimodal predictions uniformly outperform the SAR spectrum predictions. The relative importance of the banks quadrant peak in the measured spectra increases for frequencies

Table 4. Comparison of measured and predicted values of the ratio of the banks quadrant (250 to 269°T) energy to the northern window quadrant (270 to 295°T) energy at TPB. The predictions are made with the SAR spectrum, $E_r(\alpha)$, and the unimodal approximation, $E_u(\alpha)$. Three estimates are used to obtain the ratio from the array data

	Banks/window energy ratio					
		Predicted			Measured	
	Frequency (Hz)	$E_r(\alpha)$	$E_u(\alpha)$	IMLM	MSEM	MLM
25 March	0.082	109.0	59.2	18.2	21.9	25.4
	0.090	41.5	17.1	17.1	19.8	26.6
	0.098	93.9	15.4	19.6	17.2	28.2
	0.106	79.5	6.8	24.2	29.3	29.6
	0.114	77.3	5.4	31.9	29.4	35.3
	Average	80.2	20.8	22.2	23.5	29.0
28 March	0.082	136.0	16.9	12.2	10.9	20.1
	0.090	136.0	4.7	8.6	9.2	15.0
	0.098	93.5	12.2	9.3	15.6	14.4
	0.106	111.0	9.8	8.6	17.8	15.5
	0.114	96.1	5.9	13.3	14.4	20.8
	Average	114.5	9.9	10.4	13.5	17.2

greater than about 0.10 Hz. This is not reflected in the unimodal predictions. Again, we suggest that this is due to the increasing importance of a background level in the true deep ocean spectrum. SNODGRASS *et al.* (1966) determined that a uniform background level ($\sim 5 \times 10^3$ cm^2 s^{-1}; compare to Fig. 5) exists for the frequency range 0.075 to 0.10 Hz. This level will become relatively important for frequencies with the least swell energy. On 25 and 28 March the high frequency limit of the swell peak does correspond with the frequency of rising importance of the banks quadrant energy.

The energy at Oceanside is not adequately predicted with either the SAR spectrum or the unimodal approximation estimates of the deep ocean spectrum. The SAR spectrum predictions severely overpredict the energy (Table 2), while the unimodal model results in a strong underprediction. The differential response to the southern and northern quadrants is more dramatic at Oceanside than at TPB, so problems with low background levels in the southern quadrant are magnified. An extremely accurate deep ocean directional spectrum is required for useful prediction of the Oceanside wave conditions.

High frequency (0.121 *to* 0.145 Hz)

The high frequency range has a large discrepancy between the data-model comparisons on 25 March and those of 28 March. There is a uniform underprediction of the band energy values on 25 March and an even larger discrepancy, with an overprediction bias, on 28 March. The size of the overprediction is greatest at 0.137 Hz, which is also the spectral maximum at the coastal sites. The Begg Rock SAR spectrum, the smeared response at TPB, and the locally measured spectrum for 0.137 Hz on 25 March are shown in Fig. 9a. The TPB spectrum is significantly greater than the predicted response and the deep ocean spectrum for most directions, the difference being most dramatic in the sector 280 to 300°T. PAWKA (1983) showed that many of the features of the directional spectrum on this day, such as a high energetic level in the San Clemente Island 'trough' (270°T) and the peak (305°T) in the sheltered north quadrant, are due to local (i.e., inside the islands) wind generation. The

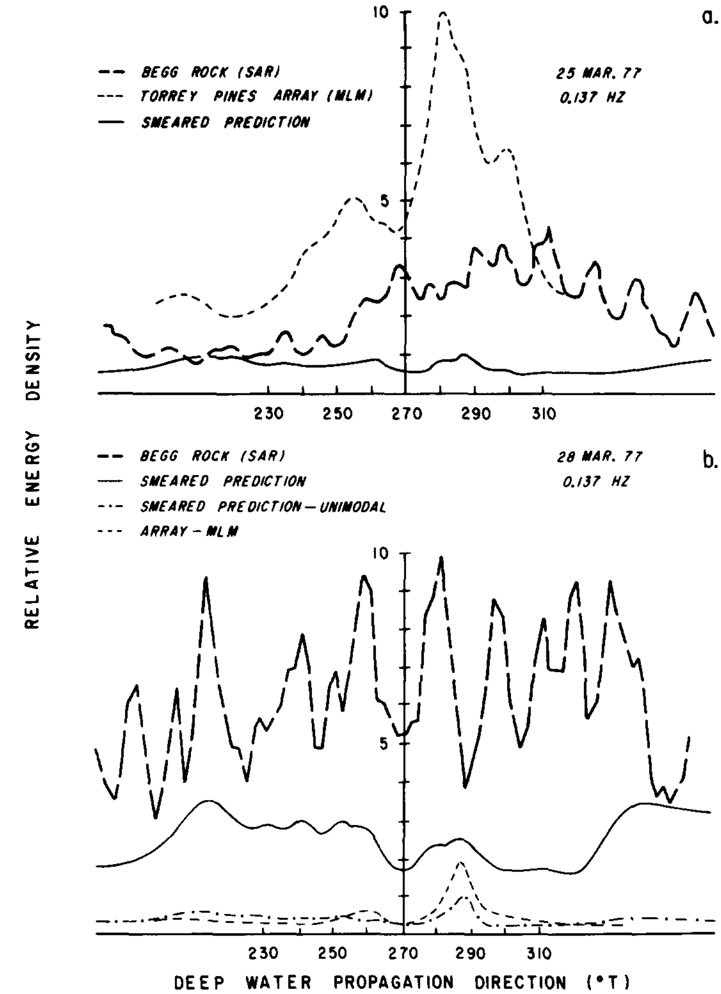

Fig. 9. Comparisons of smeared predictions of the directional spectrum with the measured spectrum at TPB. The 28 March spectrum is also compared with a smeared unimodal prediction (the unimodal approximation obtained from the wind directions). Also shown are the deep ocean (Begg Rock) SAR estimates. The spectra are normalized by a constant factor. The measured band energies for Begg Rock and TPB, respectively, are 1.5 and 2.1 × 10^4 cm^2 s^{-1} on 25 March and 5.1 and 3.6 × 10^3 cm^2 s^{-1} on 28 March.

energetic comparisons given here are consistent with strong local generation effects in the high frequency ranges.

As mentioned previously, the high frequency coastal energy level is grossly overpredicted on 28 March. There is an apparent systematic drop in energy with propagation as the coastal band energy is overpredicted by a factor of five (Table 2), while the band energy at the San Clemente Island waverider is roughly 50 to 60% of the predicted value. An example of the Begg Rock SAR spectrum for this frequency range on 28 March is plotted in Fig. 9b along with the predicted response and measured spectrum at TPB. The deep ocean spectrum shows little organized form and there is no agreement between the predicted response and the measured spectrum. In particular, the measured directional spectrum shows relatively low energy density in the quadrants 230 to 250°T and 278 to 285°T, which are completely exposed to the apparent high spectrum levels in these sectors of the deep ocean spectrum. The measured TPB spectrum peaks relatively sharply near the boundary to the north quadrant window (291°T). This is in contrast to the high frequency directional spectra sampled on 25 March.

The winds measured at San Nicolas Island on 28 March average 9 m s^{-1} with directions near 320°T. The coastal winds are significantly lighter (4 m s^{-1}) and have a shifting direction during the day. REGIER (1975) showed that the directional spectrum in a wind generated spectral peak is relatively narrow (~40°) with the mode being roughly colinear with the wind. Note the marked difference between the SAR spectrum (Fig. 9) and this unimodal model. The unimodal distribution was used as an input to the sheltering model and the resulting smeared prediction (also shown in Fig. 9b) closely matches the measured TPB spectrum. Additionally, the predicted coastal energy values using this model are within 20% of the measured values. However, this assumed directional distribution underpredicts the band energy at the San Clemente Island waverider by a factor of two. The true high frequency directional spectrum is most likely made up of components following the wind (300 to 340°T) and 'swell' near the mid-frequency mode at 295 to 300°T.

The field verification of the local wind generation effects in this region will require extensive sampling of the obviously complex wind field as well as accurate deep ocean directional spectra.

DISCUSSION

Predictions of the coastal wave field at TPB were made with a unimodal deep ocean directional spectrum input to the island refraction/blocking model. The unimodal predictions of both total band energy and directional structure (relative strength and location of directional modes) at TPB agreed well with field data in the frequency range 0.082 to 0.114 Hz. The unimodal approximations were obtained from model fits to the L-band SAR spectra. Southern swell at low frequency and local wind effects at high frequency restrict the application of the unimodal approximation to this frequency range.

Neither the SAR spectra nor the unimodal approximations of the deep ocean directional spectra yielded predictions that agreed well with the measured data at Oceanside. Severe blocking of the north swell makes the local spectrum at this site very sensitive to low background levels in the deep ocean southern quadrant. The (north swell) unimodal approximations have no energy in the southern quadrant and this is not considered to be absolutely realistic. The general quantitative verification of the island refraction/blocking model will require stable, high resolution directional spectra in the region west of the islands. A unimodal approximation of the deep ocean directional spectrum is not generally adequate for use in wave predictions on this partially sheltered coast.

It is shown that strongly bimodal directional spectra at low wave frequencies can occur at TPB in response to north swell. The southern mode, which is due to refraction of the northern swell to the site by Cortez and Tanner Banks, is occasionally the dominant peak. The low frequency refraction can theoretically supply up to 5 to 20% of the deep ocean energy that would otherwise be sheltered. The observed relative importance of the banks quadrant (southern) mode decreases with increasing frequency in the range 0.05 to 0.10 Hz in agreement with a unimodal deep ocean model. It is conjectured that the increasing relative importance of a neglected background spectral level is the cause of the subsequent rise of the southern mode for frequencies greater than about 0.10 Hz. At these frequencies, the refraction process can theoretically spread only 1% of the deep ocean energy to the site for sheltered deep ocean directions.

Wave generation by winds in the borderland region, which is not accounted for by this sheltering model, is shown to be important for frequencies >0.12 Hz in this data set. The high frequency band energy at the coast can actually exceed the deep ocean values during periods of local frontal activity. Effects of refraction over the island bathymetry are theoretically negligible for these higher wave frequencies.

Acknowledgements—The Torrey Pines Beach array data was collected under joint sponsorship of the Office of Naval Research (ONR), Code 422CS (Coastal Sciences), Contract N00014-75-C-0300, and the Jet Propulsion Laboratory (JPL). ONR funded the analysis under the same contract. R. LOWE and the staff at the Shore Processes Laboratory installed the array and retrieved the data. O. SHEMDIN and S. V. HSIAO at JPL supplied the SAR data. R. SEYMOUR at Scripps Institution of Oceanography collected and analyzed the Oceanside pressure data. A. REECE at the Shell Development Company provided the Tanner Bank wave staff and current meter data. MIKE CLARK drafted the figures and JOAN SEMLER typed the manuscript. The first author wishes to address a special note of appreciation to RICHARD ANDERSON, M.D. and AL WEINBERG for their part in making the writing of the manuscript possible.

REFERENCES

ARTHUR R. S. (1951) The effect of islands on surface waves. *Scripps Institution of Oceanography Bulletin*, **6**, 1–26.

CAPON J. (1969) High-resolution frequency-wavenumber spectrum analysis. *Proceedings of the Institute of Electrical and Electronic Engineers*, **57**, 1408–1418.

COLLINS J. I. (1972) Prediction of shallow-water spectra. *Journal of Geophysical Research*, **77**, 2693–2707.

DOBSON R. S. (1967) Some applications of digital computer to hydraulic engineering problems. Tech. Rep. No. 80, Department of Civil Engineering, Stanford University.

EMERY K. O. (1958) Wave patterns off Southern California. *Journal of Marine Research*, **17**, 133–140.

HOM-MA M., K. HORIKAWA and Y. CHAO (1966) Sheltering effects of Sado Island on wind waves off Niigata Coast. *Coastal Engineering in Japan*, **9**, 27–44.

LONGUET-HIGGINS M. S. (1957) On the transformation of a continuous spectrum by refraction. *Proceedings of the Cambridge Philosophical Society*, **53**, 226–229.

MUNK W. H. and R. S. ARTHUR (1952) Wave intensity along a refracted ray. In: *Gravity waves*, U.S. Department of Commerce, National Bureau of Standards, cir. 521, pp. 95–108.

MUNK W. H., G. R. MILLER, F. E. SNODGRASS and N. F. BARBER (1963) Directional recording of swell from distant storms. *Philosophical Transactions of the Royal Society of London*, **A255**, 505–584.

NATIONAL MARINE CONSULTANTS (1960) Wave statistics for seven deepwater stations along the California coast, U.S. Army Corps of Engineering, L.A. District.

PAWKA S. S. (1982) Wave directional characteristics on a partially sheltered coast. PhD Dissertation, University of California, San Diego, 246 pp.

PAWKA S. S. (1983) Island shadows in wave directional spectra. *Journal of Geophysical Research*, **88**, 2579–2591.

PAWKA S. S., S. V. HSIAO, O. H. SHEMDIN and D. L. INMAN (1980) Comparisons between wave directional spectra from SAR and pressure sensor arrays. *Journal of Geophysical Research*, **85**, 4987–4995.

PHILLIPS O. M. (1977) *The dynamics of the upper ocean*. Cambridge University Press, London, 336 pp.

REGIER L. A. (1975) Observations of the power and directional spectrum of oceanic surface waves. PhD Dissertation, University of California, San Diego, 176 pp.

SHEMDIN O. H. (1980) The West Coast Experiment: A Review. *EOS, Transactions of the American Geophysical Union*, **61**, 649–651.

SNODGRASS F. E., G. W. GROVES, K. F. HASSELMANN, G. R. MILLER, W. H. MUNK and W. H. POWERS (1966) Propagation of ocean swell across the Pacific. *Philosophical Transactions of the Royal Society of London*, **259**, 431–497.

WILSON S. W., D. G. WILSON and J. A. MICHAEL (1973) Analysis of swell near the island of Aruba. *Journal of Geophysical Research*, **78**, 7834–7844.